Biochemical and Biophysical Research Communications 431 (2013) 117–123

Contents lists available at SciVerse ScienceDirect

Biochemical and Biophysical Research Communications

journal homepage: www.elsevier.com/locate/ybbrc

Piperlongumine induces inhibition of the ubiquitin–proteasome system in cancer cells

Malin Jarvius [a,1], Mårten Fryknäs [a,1], Pädraig D'Arcy [b,1], Chao Sun [b], Linda Rickardson [a], Joachim Gullbo [a], Caroline Haglund [a], Peter Nygren [c], Stig Linder [b,*,1], Rolf Larsson [a,*,1]

[a] Department of Medical Sciences, Division of Clinical Pharmacology, Uppsala University, S-751 85 Uppsala, Sweden
[b] Department of Oncology–Pathology, Karolinska Institute, S-17176 Stockholm, Sweden
[c] Department of Radiology, Oncology and Radiation Sciences, Uppsala University, S-751 85 Uppsala, Sweden

ARTICLE INFO

Article history:
Received 28 December 2012
Available online 11 January 2013

Keywords:
Cancer therapy
Apoptosis
Proteasome
Piperlongumine
Oxidative stress

ABSTRACT

Piperlongumine, a natural product from the plant *Piper longum*, has demonstrated selective cytotoxicity to tumor cells and to show anti-tumor activity in animal models [1]. Cytotoxicity of piperlongumine has been attributed to increase in reactive oxygen species (ROS) in cancer cells. We here report that piperlongumine is an inhibitor of the ubiquitin–proteasome system (UPS). Exposure of tumor cells to piperlongumine resulted in accumulation of a reporter substrate known to be rapidly degraded by the proteasome, and of accumulation of ubiquitin conjugated proteins. However, no inhibition of 20S proteolytic activity or 19S deubiquitinating activity was observed at concentrations inducing cytotoxicity. Consistent with previous reports, piperlongumine induced strong ROS activation which correlated closely with UPS inhibition and cytotoxicity. Proteasomal blocking could not be mimicked by agents that induce oxidative stress. Our results suggest that the anti-cancer activity of piperlongumine involves inhibition of the UPS at a pre-proteasomal step, prior to deubiquitination of malfolded protein substrates at the proteasome, and that the previously reported induction of ROS is a consequence of this inhibition.

1. Introduction

The proteasome is a multi-unit protease system located in the cytoplasm and the nucleus and regulates the levels and functions of a large number of cellular proteins [2]. The 26S proteasome consists of the 20S core particle, containing proteolytic active sites, and one or two 19S regulatory particles [2]. Human cancer cells have an elevated level of proteasome activity and are more sensitive to proteasome inhibitors compared to normal cells [3]. Inhibition of the ubiquitin–proteasome system (UPS) is therefore a viable approach to cancer therapy [4,5]. Targeting the proteolytic core 20S particle has been validated in the clinical setting with the use of the proteasome inhibitor bortezomib in multiple myeloma [6].

The connectivity map (CMAP) is an open resource collection of genome-wide transcriptional expression data from cultured human cells treated with bioactive compounds [7]. CMAP contains expression signatures from more than 1300 small molecules and can be used to find connections among those compounds sharing a common mechanism of action [7]. The analysis of gene expression signatures has a major advantage in that the functional response to drugs can be assessed, i.e. those interactions between drug and targets that generate the relevant cellular response.

Recently, the specific blocking of the deubiquitinating (DUB) activity of the 19S regulatory particles (19S RP) was identified as a novel principle for proteasome inhibition using the small molecule b-AP15 as a prototype inhibitor [8]. This compound specifically interact with the deubiquitinases UCHL5 and USP14 of the 19S RP and demonstrates significant anti-tumor activity both in vitro and in vivo also in solid tumor types not sensitive to bortezomib, including colon cancer [8]. In the present study, we used CMAP to probe for compounds causing similar gene expression perturbations as b-AP15. Piperlongumine, retrieved from CMAP and not previously associated with proteasomal inhibition, demonstrated inhibition of UPS at concentrations inducing cytotoxicity. The compound induced strong ROS activation which correlated closely with accumulation of ubiquitin conjugated proteins and cytotoxicity. Our findings raise the possibility that the primary or complementary functional response to piperlongumine is inhibition of the UPS.

* Corresponding authors. Fax: +46 18519237 (R. Larsson).
E-mail addresses: stig.linder@ki.se (S. Linder), rolf.larsson@medsci.uu.se (R. Larsson).
[1] Contributed equally to this work.

0006-291X/$ - see front matter © 2013 Elsevier Inc. All rights reserved.
http://dx.doi.org/10.1016/j.bbrc.2013.01.017

2. Materials and methods

2.1. Chemicals

Piperlongumine, rotenone, phenoxybenzamine and parthenolide was purchased from Sigma–Aldrich (Stockholm, Sweden), and the proteasome inhibitor bortezomib was from LC Laboratories, Woburn, MA, USA. The 19S inhibitor b-AP15 was synthesized by OncoTargeting AB (Uppsala, Sweden) (also available from Boston Biochem, Cambridge, MA). H_2O_2 was purchased from Merck (Whitehouse Station, NJ, USA).

2.2. Cell culture

The breast cancer cell line MCF7 (American Type Culture Collection, Manassas, VA, USA) was cultured in Minimum Essential Medium Eagle with 1 mM sodium pyruvate. MelJuSo Ub^{G76V}-YFP, a human melanoma cell line expressing ubiquitin coupled to yellow fluorescent protein (YFP, [9]), was grown in Dulbecco's Modified Eagle's Medium. Colon cancer HCT116 cells were cultured in RPMI 1640 medium. All media were supplemented with 10% heat-inactivated fetal bovine serum, 2 mmol/L L-glutamine, 100 μg/mL streptomycin and 100 U/mL penicillin (all from Sigma–Aldrich). The cell lines were cultured at 37 °C in a humidified atmosphere containing 5% CO_2.

2.3. Gene expression analysis using the Connectivity Map

The drug-induced gene expression perturbations of b-AP15 were studied using the Connectivity Map (CMAP) build 02 (www.broad.mit.edu/cmap) as previously described [7]. Briefly, breast cancer MCF7 cells were plated and treated with 1 μM b-AP15 or vehicle control (DMSO) for 6 h. Details of the methods for drug exposure, RNA preparation, and gene expression analysis has been described elsewhere [7,8]). Only probes present on HG U133A Affymetrix chips were used. A gene signature consisting of the 30 most up- and down-regulated genes (i.e. probes) for each compound was used to interrogate the CMAP database to retrieve a ranked list of compounds.

2.4. Gene enrichment analysis

Enrichment analysis based on gene expression results was performed with GeneGo Metadrug software (GeneGo, Thomson Reuters [10]). The Metadrug database contains both public and proprietary functional ontologies that collect genes/proteins into biologically meaningful categories. Metadrug contains three public ontologies from the gene ontology (GO) consortium. Additionally, Metadrug includes six proprietary ontologies based on more than 2300 pathway maps and networks. Enrichment calculations uses hypergeometric distribution to calculate the probability that the degree of overlap between the list of differentially expressed genes generated by the compounds and the genes represented in the ontologies is statistically significant.

2.5. Measurement of cytotoxic activity

The cytotoxic activity of piperlongumine was measured using the fluorometric microculture cytotoxicity assay (FMCA). The method is based on measurement of fluorescence generated by hydrolysis of fluorescein diacetate (FDA) to fluorescein by cells with intact plasma membranes [11]. In brief, 6000 MelJuSo Ub^{G76V}-YFP cells per well were seeded into 96-well microplates and incubated over night before treatment with 2.5–20 μM piperlongumine. The plates were incubated at 37 °C for 72 h, and then washed and FDA was added to the wells followed by 50 min of incubation at 37 °C. The fluorescence, which is proportional to the number of living cells in each well, was measured at 485/520 nm in a Fluoroskan instrument (Labsystems, GMI, Ramsey, MIN). Cell survival is presented as survival index (SI), defined as the fluorescence value in the compound-treated wells analyzed as percentage of the value in the control wells, with blank values subtracted. Quality criteria included a signal/blank ratio >10 and a coefficient of variation (CV) in control and blank wells <30.

2.6. Live-cell analysis of UPS-activity

MelJuSo Ub^{G76V}-YFP cells (6000 cells/well) were plated in black optically clear bottom 96-well ViewPlates (PerkinElmer, Waltham, MA, USA) over-night and then treated with 2.5–20 μM piperlongumine, 1 μM bortezomib, 1 μM b-AP15, 10 μM and 50 μM rotenone and 1 mM H_2O_2. Treatment with compounds that block the UPS leads to accumulation of YFP in these cells, and the generated fluorescence was continuously detected in an IncuCyte FLR instrument (Essen BioScience Inc., Ann Arbor, MI) that captures images of the cells over time.

2.7. Analysis of poly-ubiquitinated proteins

Cells were lysed with ice-cold NP-40 lysis buffer (50 mM Tris–HCl, pH 7.4, 0.15 M NaCl, 1.0 mM EDTA, 1% NP-40) freshly supplemented with protease cocktail inhibitors (Sigma–Aldrich), 10 mM *N*-ethylmaleimide (NEM; EMD Chemicals) and 2 mM iodoacetic acid (IAA; Sigma–Aldrich). Lysates were cleared by centrifugation at 13,000*g* for 15 min at 4 °C and the protein concentration was measured by the Bradford (Bio-Rad, Richmond, CA, USA) assay. Proteins (10 μg) were denatured under reducing conditions (1% β-mercaptho-ethanol) in NuPAGE sample buffer (Invitrogen, Carlsbad, CA) and resolved by Tris-Acetate PAGE gels (Invitrogen). For the purpose of detection of Ub^{G76V}-YFP, proteins were analyzed on 4–12% gradient gels, while detection of ubiquitin-conjugated proteins was performed using 3–8% gradient gels. Proteins were transfered onto polyvinylidene difluoride (PVDF; Hybond-P, Amersham, UK) membranes. Membranes were stained with 0.1% Ponceau to visualize equal loading and homogeneous transfer. After blocking the membranes with 5% non-fat dry milk (Bio-Rad) in TBS-0.05% Tween-20, proteins of interest were detected using mAb followed by peroxidase-labeled sheep anti-mouse IgG or donkey anti-rabbit IgG and a chemiluminescence reaction (ECL; Amersham). Anti-UbK48 (Apu2; Millipore, Temecula, California) and anti-GFP (B-2; Santa Cruz Biotechnology, Heidelberg, Germany) antibodies were used at 1:1000 dilutions. Mouse anti-β-actin primary antibody obtained from Sigma–Aldrich was used at 1:5000 dilution.

2.8. Measurement of proteasome activity and deubiquitinase activity

In vitro proteasome activity assays were performed using 26S proteasomes (Boston Biochem, Cambridge, MA) in reaction buffer (25 mM Hepes, 50 mM NaCl, 10 mM $MgCl_2$, 2 mM ATP, 1 mM DTT). We used 10 μM Suc-LLVY-AMC (Boston Biochem) for the detection of chymotrypsin-like proteasome activity using Wallac Multilabel counter equipped with 380 nm excitation and 460 nm emission filters. For DUB inhibition assays, 26S proteasome (5 nM) or total HCT116 cell lysates were incubated with DMSO, piperlongumine or b-AP15 and cleavage of ubiquitin-AMC (1 μM) was monitored.

2.9. Measurement of oxidative stress

Oxidative stress was assessed using the Cellomics Oxidative Stress I Kit containing dihydroethidium (DHE) probe and Hoechst 33342 (Thermo Fischer Scientific, Rockford, IL,USA) according to the manufacturer's instructions. The principle of the method is that reactive oxygen species convert non-fluorescent DHE to fluorescent ethidium which subsequently intercalates into DNA. Hoechst 33342 is used to identify the nuclei of individual cells and ethidium fluorescence is subsequently measured to evaluate whether oxidative stress has occurred. MelJuSo Ub^{G76V}-YFP cells (6000 cells/well) were plated in black optically clear bottom 96-well ViewPlates (PerkinElmer, Waltham, MA, USA) over-night and then treated with 2.5–20 μM piperlongumine or 10 μM rotenone for 24 h before staining. Processed plates were loaded in an ArrayScan VTI (Thermo Fischer Scientific) and analyzed using the standard Hoechst and rhodamine filter setting. Images were acquired for each fluorescence channel, using suitable filters with 20× objective and in each well at least 1000 cells were analyzed. Quantification of oxidative stress performed by measuring the average intensity of fluorescent ethidium intercalated in the cell nuclei.

3. Results

A gene-expression signature of the response to the deubiquitinase inhibitor b-AP15 was generated as previously described [8]. To be compatible with the CMAP data base, MCF7 breast cancer cells were exposed to b-AP15 at 1 μM for 6 h and the gene expression profile was compared to vehicle-treated control (Fig. 1A). The gene signature obtained was used to interrogate the CMAP data base for compounds that induce similar expression patterns. A similarity score of 0.8 was used as the cut-off criterion. CMAP returned a list of compounds, including the previously characterized deubiquitinase inhibitor 15-δ prostaglandin J2 [12] and a number of compounds previously shown to be inhibitors of the proteolytic activity of the 20S subunit such as celastrol [13], withaferin A [14], MG-262 and MG-132 [15]. The search also identified the compounds piperlongumine, partenolide and phenoxybenzamine, which have not previously been associated with proteasome inhibition. A detailed analysis of the expression profiles induced by piperlongumine and phenoxybenzamine using the Metadrug software showed that both compounds induced a clear unfolded-protein response similar to that of b-AP15 (Fig. 1B).

We determined the effect of phenoxybenzamine, partenolide and piperlongumine on UPS function using a reporter cell line, MelJuSo Ub^{G76V}-YFP, expressing a proteasome-targeted fusion protein [9]. The Ub^{G76V}-YFP reporter substrate is intrinsically unstable due to constitutive degradation by the proteasome, thus impairment of the UPS leads to an increased fluorescent signal. We found that piperlongumine (Fig. 2A and B), but not partenolide or phenoxybenzamine (data not shown), induced strong accumulation of the fluorescent substrate in the reporter cell line. The accumulation of the Ub^{G76V}-YFP protein was continuously monitored using fluorescence microscopy where an increase in YFP signal was observed already after 2 h at 20 μM, reached a maximum after 12–15 h, followed by a slow decline of cellular fluorescence (Fig. 2B) coinciding with apparent morphological signs of cell death. The kinetics of accumulation of Ub^{G76V}-YFP in piperlongumine-treated cells was similar to the kinetics observed with the deubiquitinase inhibitor b-AP15 and the proteasome inhibitor bortezomib (Fig. 2C). FMCA measurements confirmed the cytotoxic activity at this concentration range (Fig. 2D). Unexposed cells showed neither signs of UPS inhibition nor cell death at the investigated time points. We confirmed that the increase in fluorescence intensity was due to accumulation of the Ub^{G76V}-YFP reporter by western blot analysis (Fig. 2E).

The inhibition of proteasome function in living cells by piperlongumine is expected to lead to an accumulation of poly-ubiquitinated proteins in cells. This prediction was confirmed using western blotting with an ubiquitin antibody (Fig. 3A). Interestingly, the poly-ubiquitinated proteins were of higher molecular weight compared to those found in bortezomib-exposed cells, but similar to cells exposed to b-AP15 (Fig. 3A). Poly-ubiquitin chains, linked to protein substrates, are known to be trimmed from their distal ends by the proteasomal deubiquitinases USP14 and UCHL5 prior to commitment to degradation [16]. The observation of high-molecular-weight poly-ubiquitinated proteins in piperlongumine-treated cells suggested that piperlongumine inhibits the UPS at a step upstream from proteasomal degradation, either prior to trimming of poly-ubiquitin chains by USP14/UCHL5 or by direct inhibition of these enzymes. We indeed found that piperlongumine did

A

rank	CMAP name	dose	cell	score
1	MG-262	100 nM	MCF7	1
2	15-δ prostaglandin J2	10 μM	MCF7	.999
3	celastrol	3 μM	MCF7	.966
4	15-δ prostaglandin J2	10 μM	MCF7	.940
5	withaferin A	1 μM	MCF7	.922
6	phenoxybenzamine	12 μM	MCF7	.915
7	phenoxybenzamine	12 μM	MCF7	.915
8	phenoxybenzamine	12 μM	MCF7	.900
9	15-δ prostaglandin J2	10 μM	MCF7	.890
10	15-δ prostaglandin J2	10 μM	MCF7	.889
11	piperlongumine	13 μM	MCF7	.874
12	15-δ prostaglandin J2	10 μM	MCF7	.873
13	partenolide	16 μM	MCF7	.859
14	15-δ prostaglandin J2	10 μM	MCF7	.847
15	MG-132	21 μM	MCF7	.835
16	15-δ prostaglandin J2	10 μM	PC3	.831
17	MG-262	100 nM	PC3	.828
18	thiostrepton	2 μM	MCF7	.817

B

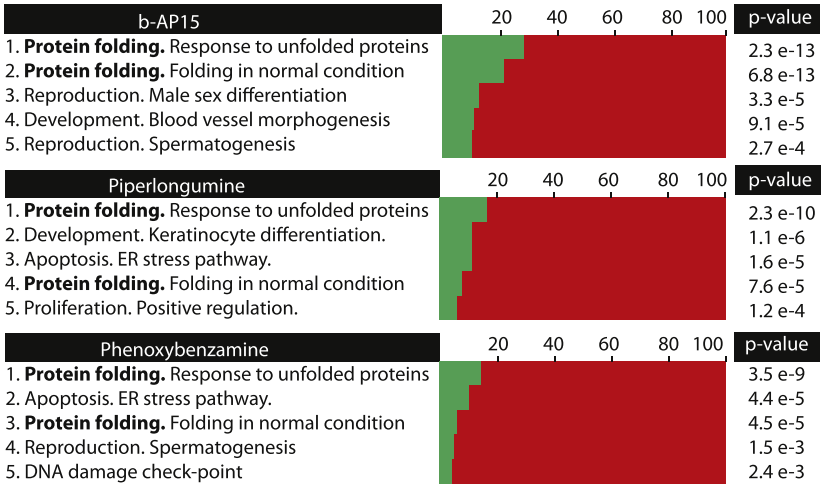

Fig. 1. Piperlongumine induces a gene expression pattern similar to inhibitors of the ubiquitin–proteasome system. (A) Connectivity Map (CMAP) results based on b-AP15 exposed MCF7 cells. All compounds except phenoxybenzamine, piperlongumine and parthenolide have previously been described as inhibitors of the UPS system. Score according to the CMAP database [7]. (B) Enrichment analysis for up-regulated genes (fraction of genes in each category found to be upregulated by >2-fold) in response to b-AP15, piperlongumine and phenoxybenzamine. For details, see Section 2 and ref. [10]. The negative log of the *p*-value from the hypergeometric distribution calculation is also presented.

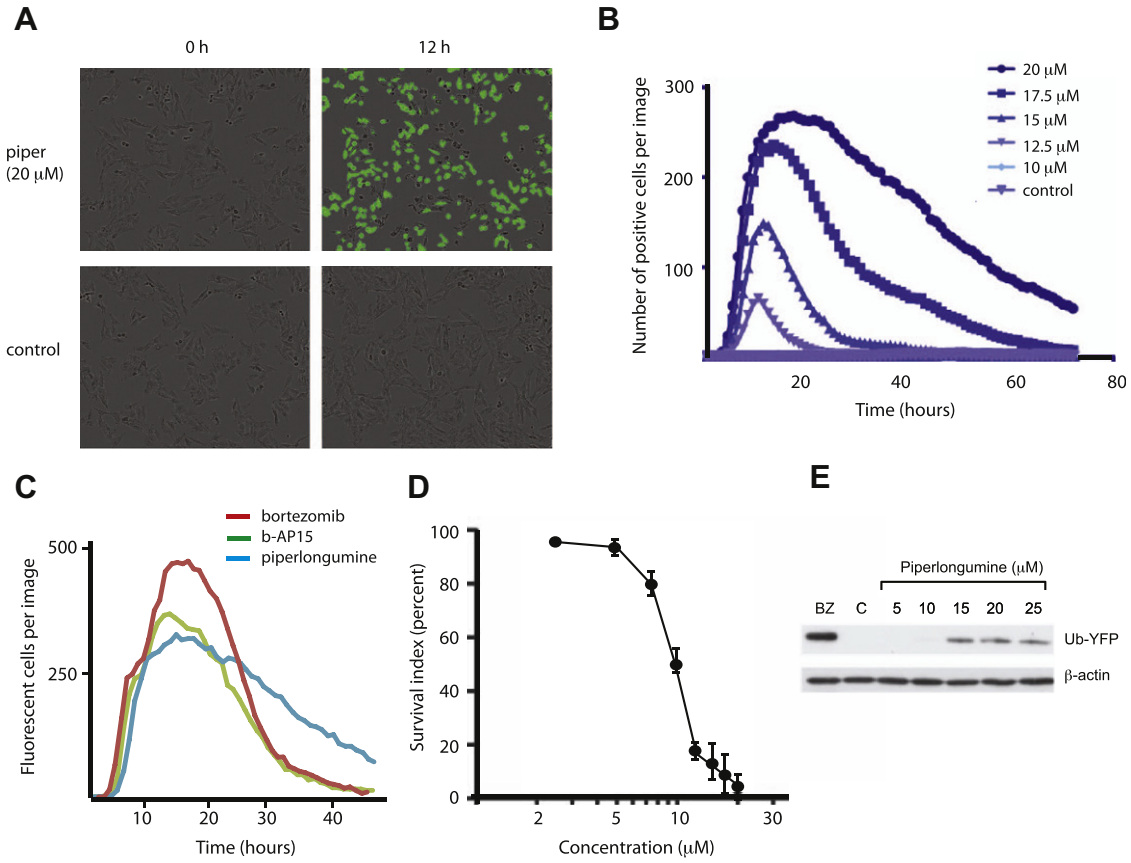

Fig. 2. Piperlongumine blocks the ubiquitin–proteasome system. (A) Accumulation of Ub-YFP in MelJuSo cells 12 h after addition of 20 –M piperlongumine compared to DMSO control. (B) Quantification of accumulated Ub-YFP in MelJuSo cells treated with increasing concentrations of piperlongumine. (C) Kinetics of Ub-YFP accumulation after treatment with 1 μM bortezomib, 1 μM b-AP15 and 20 μM piperlongumine. A–C are monitored in an Incucyte FLR instrument. (D) Cytotoxic activity of piperlongumine in MelJuSo cells using the FMCA viability assay. Data is expressed as mean values (±SEM) of four separate experiments. (E) Ub-YFP accumulation by piperlongumine was confirmed using western blotting.

not to inhibit proteasome activity (Fig. 3B), consistent with this line of reasoning.

In order to address the possibility that piperlongumine has a molecular mechanism of action similar to that of b-AP15, i.e. inhibition of proteasomal deubiquitinases, we examined deubiquitinase activity of purified 19S proteasomes. We did not, however, observe inhibition of proteasome-associated ubiquitin-AMC cleavage activity by piperlongumine, even at high concentrations. This was in contrast to b-AP15 which inhibited proteasome-associated deubiquitinase activity (Fig. 3C). Furthermore, piperlongumine did not inhibit total cellular deubiquitinase activity in cell lysates (Fig. 3D).

Consistent with previous reports [1,17], a concentration-dependent induction of ROS was observed after exposure of cells to piperlongumine (Fig. 4A) which closely correlated to piperlongumine-induced cytotoxicity (Fig. 4B). Cytotoxicity was also closely associated with accumulation of the Ub^{G76V}-YFP reporter (Figs. 2 and 4C). We considered the possibility that induction of ROS by piperlongumine might lead to secondary inhibition of the UPS. However, pharmacological induction of ROS using rotenone or by direct addition of H_2O_2 could not mimic the Ub^{G76V}-YFP reporter accumulation caused by piperlongumine (Fig. 4D), making this explanation less likely.

4. Discussion

Piperlongumine was recently described to selectively kill cancer cells by reducing the levels of glutathione S-transferase-Π (GSTP1) and carbonyl reductase 1 (CBR1), resulting in ROS formation and a DNA damage response, subsequently leading to mitochondrial apoptosis [1]. The present study adds to these previous observations in demonstrating a functional proteasomal blocking in cells, as evidenced by inhibition of degradation of a ubiquitin fusion protein and strong accumulation of poly-ubiquitinated proteins in piperlongumine-exposed cells. Importantly, proteasomal blocking was observed at cytotoxic drug concentrations. Piperlongumine did not, however, inhibit proteasome enzymatic degradation activity. The molecular weights of poly-ubiquitinated proteins accumulating in piperlongumine-treated cells were higher than those observed in cells treated with bortezomib, an inhibitor of 20S enzyme activity. Similar observations were previously reported for the USP14/UCHL5 deubiquitinase inhibitor b-AP15, and are expected from inhibition of the USP14/UCHL5 deubiquitinases of the 19S proteasome subunit [8,18]. We did not, however, observe inhibition of 19S proteasomal deubiquitinase activity by piperlongumine. The exact mechanism of how piperlongumine inhibits the UPS is therefore unclear. Since ubiquitin residues are removed from the tips of poly-ubiquitin chains after binding to the proteasome, we believe it likely that piperlongumine affects a pre-proteasomal step of protein processing. Proteins extracted from the ER by the ERAD system are presented to the proteasome by UBA-UBL containing proteins such as ubiquilin-1, Rad23 and Dsk2 (see [19]). Furthermore, mislocalized membrane proteins (MLPs) are captured by the Bag6 complex for subsequent degradation [20]. Interference of critical steps in these pre-proteasomal pathways are likely to result in a phenotype similar to that observed

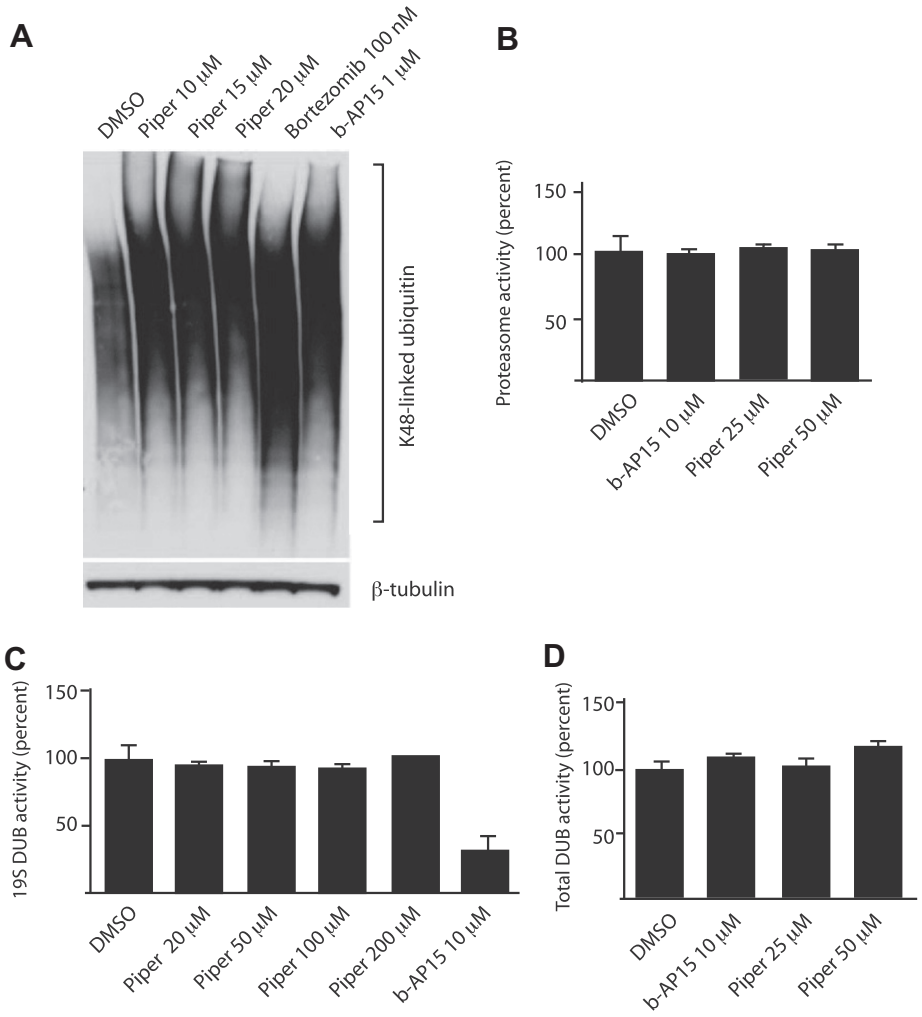

Fig. 3. Piperlongumine induces accumulation of poly-ubiquitin conjugates without inhibition of the proteasome. (A) HCT116 cells were exposed to the indicated concentrations of piperlongumine for 6 h. Lysates from cells were prepared for western blotting and probed using antibodies to K48-linked polyubiquitin or tubulin. (B) Proteasome activity was measured using Suc-LLVY-AMC as substrate. Piperlongumine was added at different concentrations and bortezomib was used as a positive control. (C) Purified recombinant 19S RP (10 nM, Boston Biochem) was incubated with the indicated concentrations of piperlongumine and deubiquitinase activity was measured by monitoring cleavage of Ub-AMC. (D) Total cell extracts from HCT116 cells were incubated with the indicated concentrations of piperlongumine and deubiquitinase activity was measured by monitoring cleavage of Ub-AMC.

in piperlongumine-treated cells, i.e. accumulation of high-molecular weight ubiquitinated proteins. It should be noted, however, that piperlongumine does block degradation of Ub^{G76V}-YFP. The step affected by the drug is therefore likely to be coupled to proteasomal degradation.

We observed a close correlation between ROS generation, cytotoxicity and functional proteasome blocking. Our results raise two alternative possibilities to explain piperlongumine-induced cell death. The compound could directly target important components of the UPS leading to secondary generation of ROS. It is well known that classical 20S inhibitors such as bortezomib and MG-262 increase ROS formation, potentially due to stabilization of critical regulators of oxidative stress [21]. Alternatively, inhibition of the UPS may due to ROS generation and alkylation of cysteine residues present in components of the UPS. ROS per se has, indeed, previously been shown to inhibit the ATP-dependent 19S activity in cell free systems [22,23], providing a mechanism to explain the UPS inhibitory activity of piperlongumine. However, induction of ROS by rotenone or by adding H_2O_2 did not cause proteasome blocking judged by measuring Ub^{G76V}-YFP accumulation. Furthermore, the kinetics of Ub^{G76V}-YFP accumulation was similar in cells treated with the 20S inhibitor bortezomib and b-AP15 (Fig. 2C), a finding not consistent with piperlongumine-induced proteasome blocking being a secondary event. Finally, other agents which are known to generate cellular ROS, such as anthracycline anti-cancer drugs [24], do not generate proteasome inhibitor-type gene expression profiles [25]. We therefore suggest that the primary or complementary functional response to piperlongumine is inhibition of the UPS, and that ROS generation is a secondary effect.

The query signature used to discover piperlongumine in CMAP was derived from b-AP15, a recently described inhibitor of the cysteine deubiquitinases of the 19S proteasomal subunit. This prototype 19S inhibitor contains unsaturated ketones and two sterically accessible carbons, suggested to be the active chemical pharmacophore responsible for enzyme inhibition [8]. This pharmacophore is shared by the deubiquitinase inhibitor 15-δ prostaglandin J2 and also by piperlongumine. Interestingly, this structural element is present in many of the top compounds returned by CMAP using the b-AP15 signature as the query. Several of these compounds, including b-AP15 and 15-δ prostaglandin J2, map to the same response region (the Q-region) of self-organizing maps used to cluster the tumor cell line screening data performed by the National Cancer Institute [26]. The Q-region has been previously identified as unique compared to the cytotoxic response pro-

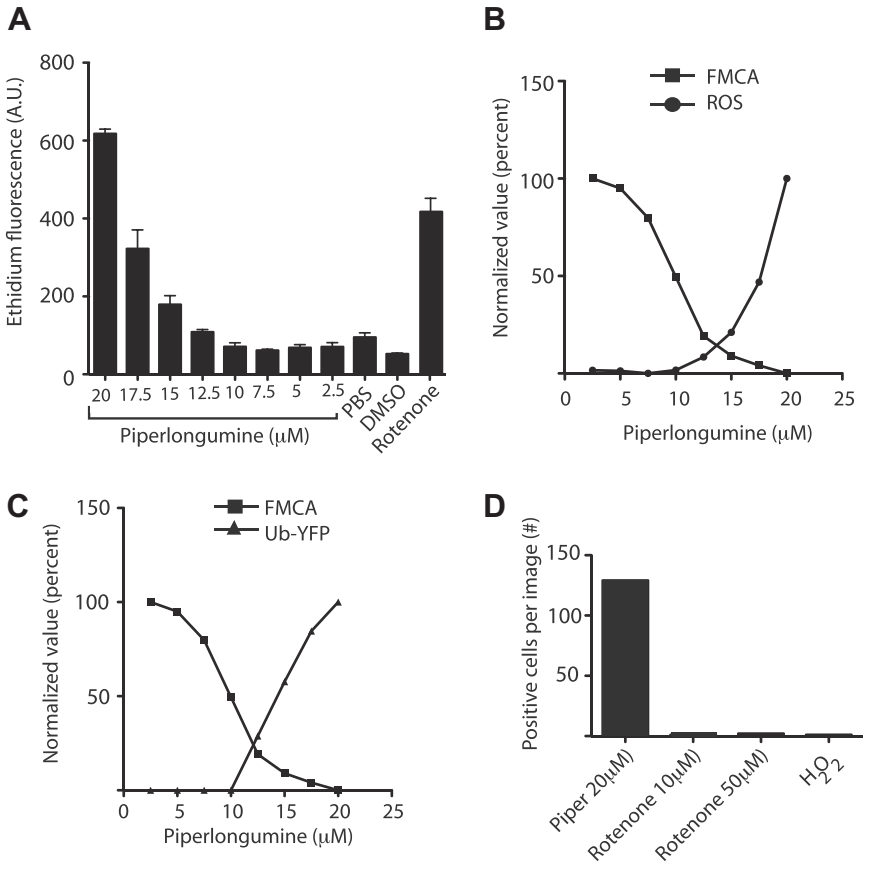

Fig. 4. Piperlongumine induces oxidative stress at cytotoxic concentrations in MelJuSo cells. (A) Cells were incubated in the presence of the indicated concentrations of piperlongumine or 10 μM of the positive control rotenone for 24 h and the levels of fluorescent ethidium in the nucleus was determined using Arrayscan VTI. The data are expressed as mean values (±SD) of two experiments with triplicate wells for each condition (B) Correlation between ROS generation and viability in response to piperlongumine. The levels of fluorescent nuclear ethidium were determined at 24 h and cell viability at 72 h. (C) Correlation between cell viability and Ub-YFP in response to piperlongumine. The accumulated Ub-YFP was determined at 12 h and cell viability at 72 h. (D) Effect of piperlongumine, rotenone and H_2O_2 on accumulation of Ub-YFP in MelJuSo cells (expressed as number of YFP positive cells per image at 12 h).

files of the entire NCI screening database. One study revealed potentially important mechanisms related to protein degradation and regulation of oxidative stress in this region [27].

The data presented here show that the major response to piperlongumine is similar to the response to proteasome inhibitors. We indeed find both functional proteasome blocking using a proteasome reporter substrate and accumulation of poly-ubiquitinated proteins. Our data raise the possibility that the previously reported induction of ROS by piperlongumine is at least partly, or even entirely, due to proteasome inhibition.

Financial support

This study was supported by the Swedish Cancer Society (S.L., P.N. and R.L.), the Swedish Research Council (S.L.), the L Eriksson Fund (M.J.) and the Lions Cancer Research Fund (P.N., M.F. and R.L.).

Acknowledgments

We are grateful for all the work with microarray array analysis at the Uppsala Expression Array Platform. The skillful technical assistance of Christina Leek and Lena Lenhammar is gratefully acknowledged.

References

[1] L. Raj, T. Ide, A.U. Gurkar, M. Foley, M. Schenone, X. Li, N.J. Tolliday, T.R. Golub, S.A. Carr, A.F. Shamji, A.M. Stern, A. Mandinova, S.L. Schreiber, S.W. Lee, Selective killing of cancer cells by a small molecule targeting the stress response to ROS, Nature 475 (2011) 231–234.

[2] M.H. Glickman, A. Ciechanover, The ubiquitin–proteasome proteolytic pathway: destruction for the sake of construction, Physiol. Rev. 82 (2002) 373–428.

[3] L. Chen, K. Madura, Increased proteasome activity, ubiquitin-conjugating enzymes, and eEF1A translation factor detected in breast cancer tissue, Cancer Res. 65 (2005) 5599–5606.

[4] J. Adams, Proteasome inhibition: a novel approach to cancer therapy, Trends Mol. Med. 8 (2002) S49–54.

[5] J. Adams, The proteasome: a suitable antineoplastic target, Nat. Rev. Cancer 4 (2004) 349–360.

[6] P.G. Richardson, W. Xie, C. Mitsiades, A.A. Chanan-Khan, S. Lonial, H. Hassoun, D.E. Avigan, A.L. Oaklander, D.J. Kuter, P.Y. Wen, S. Kesari, H.R. Briemberg, R.L. Schlossman, N.C. Munshi, L.T. Heffner, D. Doss, D.L. Esseltine, E. Weller, K.C. Anderson, A.A. Amato, Single-agent bortezomib in previously untreated multiple myeloma: efficacy, characterization of peripheral neuropathy, and molecular correlations with response and neuropathy, J. Clin. Oncol. 27 (2009) 3518–3525.

[7] J. Lamb, E.D. Crawford, D. Peck, J.W. Modell, I.C. Blat, M.J. Wrobel, J. Lerner, J.P. Brunet, A. Subramanian, K.N. Ross, M. Reich, H. Hieronymus, G. Wei, S.A. Armstrong, S.J. Haggarty, P.A. Clemons, R. Wei, S.A. Carr, E.S. Lander, T.R. Golub, The Connectivity Map: using gene-expression signatures to connect small molecules, genes, and disease, Science 313 (2006) 1929–1935.

[8] P. D'Arcy, S. Brnjic, M.H. Olofsson, M. Fryknas, K. Lindsten, M. De Cesare, P. Perego, B. Sadeghi, M. Hassan, R. Larsson, S. Linder, Inhibition of proteasome deubiquitinating activity as a new cancer therapy, Nat. Med. 17 (2011) 1636–1640.

[9] V. Menendez-Benito, L.G. Verhoef, M.G. Masucci, N.P. Dantuma, Endoplasmic reticulum stress compromises the ubiquitin–proteasome system, Hum. Mol. Genet. 14 (2005) 2787–2799.

[10] R.J. Brennan, T. Nikolskya, S. Bureeva, Network and pathway analysis of compound–protein interactions, Methods Mol. Biol. 575 (2009) 225–247.

[11] E. Lindhagen, P. Nygren, R. Larsson, The fluorometric microculture cytotoxicity assay, Nat. Protoc. 3 (2008) 1364–1369.

[12] J.E. Mullally, P.J. Moos, K. Edes, F.A. Fitzpatrick, Cyclopentenone prostaglandins of the J series inhibit the ubiquitin isopeptidase activity of the proteasome pathway, J. Biol. Chem. 276 (2001) 30366–30373.

[13] H. Yang, D. Chen, Q.C. Cui, X. Yuan, Q.P. Dou, Celastrol, a triterpene extracted from the Chinese "Thunder of God Vine", is a potent proteasome inhibitor and suppresses human prostate cancer growth in nude mice, Cancer Res. 66 (2006) 4758–4765.

[14] H. Yang, G. Shi, Q.P. Dou, The tumor proteasome is a primary target for the natural anticancer compound Withaferin A isolated from "Indian winter cherry", Mol. Pharmacol. 71 (2007) 426–437.

[15] J. Adams, M. Behnke, S. Chen, A.A. Cruickshank, L.R. Dick, L. Grenier, J.M. Klunder, Y.T. Ma, L. Plamondon, R.L. Stein, Potent and selective inhibitors of the proteasome: dipeptidyl boronic acids, Bioorg. Med. Chem. Lett. 8 (1998) 333–338.

[16] M.J. Lee, B.H. Lee, J. Hanna, R.W. King, D. Finley, Trimming of ubiquitin chains by proteasome-associated deubiquitinating enzymes, Mol. Cell Proteomics 10 (2011). R110 003871.

[17] D.J. Adams, M. Dai, G. Pellegrino, B.K. Wagner, A.M. Stern, A.F. Shamji, S.L. Schreiber, Synthesis, cellular evaluation, and mechanism of action of piperlongumine analogs, Proc. Natl. Acad. Sci. USA 109 (2012) 15115–15120.

[18] P. D'Arcy, S. Linder, Proteasome deubiquitinases as novel targets for cancer therapy, Int. J. Biochem. Cell Biol. 44 (2012) 1729–1738.

[19] P.J. Lim, R. Danner, J. Liang, H. Doong, C. Harman, D. Srinivasan, C. Rothenberg, H. Wang, Y. Ye, S. Fang, M.J. Monteiro, Ubiquilin and p97/VCP bind erasin, forming a complex involved in ERAD, J. Cell Biol. 187 (2009) 201–217.

[20] T. Hessa, A. Sharma, M. Mariappan, H.D. Eshleman, E. Gutierrez, R.S. Hegde, Protein targeting and degradation are coupled for elimination of mislocalized proteins, Nature 475 (2011) 394–397.

[21] J. Chandra, Oxidative stress by targeted agents promotes cytotoxicity in hematologic malignancies, Antioxid. Redox Signaling 11 (2009) 1123–1137.

[22] T. Shibata, T. Yamada, M. Kondo, N. Tanahashi, K. Tanaka, H. Nakamura, H. Masutani, J. Yodoi, K. Uchida, An endogenous electrophile that modulates the regulatory mechanism of protein turnover: inhibitory effects of 15-deoxy-Delta 12,14-prostaglandin J2 on proteasome, Biochemistry 42 (2003) 13960–13968.

[23] T. Ishii, T. Sakurai, H. Usami, K. Uchida, Oxidative modification of proteasome: identification of an oxidation-sensitive subunit in 26 S proteasome, Biochemistry 44 (2005) 13893–13901.

[24] K.J. Davies, J.H. Doroshow, Redox cycling of anthracyclines by cardiac mitochondria. I. Anthracycline radical formation by NADH dehydrogenase, J. Biol. Chem. 261 (1986) 3060–3067.

[25] S. Hassan, D. Laryea, H. Mahteme, J. Felth, M. Fryknas, W. Fayad, S. Linder, L. Rickardson, J. Gullbo, W. Graf, L. Pahlman, B. Glimelius, R. Larsson, P. Nygren, Novel activity of acriflavine against colorectal cancer tumor cells, Cancer Sci. 102 (2011) 2206–2213.

[26] A.A. Rabow, R.H. Shoemaker, E.A. Sausville, D.G. Covell, Mining the National Cancer Institute's tumor-screening database: identification of compounds with similar cellular activities, J. Med. Chem. 45 (2002) 818–840.

[27] D.G. Covell, A. Wallqvist, R. Huang, N. Thanki, A.A. Rabow, X.J. Lu, Linking tumor cell cytotoxicity to mechanism of drug action: an integrated analysis of gene expression, small-molecule screening and structural databases, Proteins 59 (2005) 403–433.